Emergence of correlated optics in one-dimensional waveguides for classical and quantum atomic gases

Janne Ruostekoski[1] and Juha Javanainen[2]

[1] *Mathematical Sciences, University of Southampton, Southampton SO17 1BJ, United Kingdom*
[2] *Department of Physics, University of Connecticut, Storrs, Connecticut 06269-3046*

(Dated: July 21, 2016)

We analyze the emergence of correlated optical phenomena in the transmission of light through a waveguide that confines classical or ultracold quantum degenerate atomic ensembles. The conditions of the correlated collective response are identified in terms of atom density, thermal broadening, and photon losses by using stochastic Monte-Carlo simulations and transfer matrix methods of transport theory. We also calculate the "cooperative Lamb shift" for the waveguide transmission resonance, and discuss line shifts that are specific to effectively one-dimensional waveguide systems.

Confining the light in a region comparable with the atomic scattering cross section can considerably enhance atom-light coupling and lead to new regimes of light-matter interactions. Guided modes of 1D waveguides [1] and nanofibers [2, 3] open up new avenues of optical physics where light propagation could potentially be employed in high-precision spectroscopy [4], quantum networks, light circuitry, and quantum switches [5–7]. For instance, superradiance of atoms confined inside a photonic crystal waveguide was recently reported [8], and 1D waveguides support long-range light-mediated interactions with also the possibility of creating novel quantum many-body phases [9] for atoms and light. Atomic waveguides also have close analogies in other 1D electrodynamics realizations, such as with different nanoemitter systems [10–13], surface plasmon nanowires [5], coupled cavity-QED [14], and superconducting transmission lines [7, 15].

In anticipation of the importance of many-atom physics in waveguide systems, we raise here the question: when do the atoms respond to light independently, as in an ordinary optical medium, and when is the response correlated? In an ideal 1D waveguide the light emitted by an atom travels unattenuated with a constant amplitude, and one might think that the corresponding infinite-range radiative dipole-dipole (DD) interaction sets up global correlations between the atoms. Maybe surprisingly it is not so, and the (line) density of the atoms makes a difference. We find that for randomly distributed atoms the point of demarkation is the wave number of resonant light k. At low density, the propagation delays in the multiple scattering of light between the atoms are sufficiently random that the atoms, in fact, transmit light basically independently, whereas at high density the propagation delays, being small, cannot be altogether random, and light-induced correlations emerge. This is an interesting analogy with 3D systems, where it has been found that when the typical interatomic separation is comparable or less than $1/k$, the atomic gas can exhibit a correlated response and the traditional electrodynamics fails [16]. An unambiguous observation of correlated optics has proven elusive in 3D gases, however, so 1D systems may offer a promising alternative.

The onset of emergent correlations is characterized not only in terms of atom density, but also imperfections of the waveguide such as the fraction of light radiated by the atoms that leaks out of the waveguide, and Doppler broadening of the resonance resulting from the thermal velocity distribution. We point out that the collective behavior in 1D entails a shift of the resonance line proportional to the line density of atoms. The 3D analog here are line shifts proportional to volume density, which are a well-known complication in high-precision spectroscopy. For quantum degenerate (not randomly distributed) atoms the light-induced correlations remain stronger and we find, e.g., that fermionic atom statistics leads to resonance linewidth narrowing and suppressed superradiance.

In the following, for our analysis we develop a quantum-mechanical theoretical framework for light propagation in classical and quantum degenerate atomic ensembles in 1D waveguides. Classical electrodynamics simulations provide exact solutions within the model of two-level, weakly excited, stationary atoms. An especially elegant representation of light-induced correlations is obtained using transfer matrices where we adapt theoretical methods of localization analysis in transport phenomena [17] that were originally developed for 1D electric conductivity.

We assume a narrow waveguide where the forward and backward propagating modes are determined by the wavenumber q and the polarization components $\hat{\mathbf{u}}_{q\sigma}(\boldsymbol{\varrho})$, with $\int d^2\varrho\, \hat{\mathbf{u}}^*_{q\sigma}(\boldsymbol{\varrho})\cdot\hat{\mathbf{u}}_{q\sigma}(\boldsymbol{\varrho}) = 1$; the propagation direction is denoted x, and the transverse coordinate by $\boldsymbol{\varrho}$. We describe the interactions of light and atoms in the *length* gauge that is obtained by the Power-Zienau-Woolley transformation [18]. The positive frequency component of the electric displacement $\mathbf{D}^+(\mathbf{r})$ then reads

$$\mathbf{D}^+(\mathbf{r}) = \sum_{q,\sigma} \zeta_q \hat{\mathbf{u}}_{q\sigma}(\boldsymbol{\varrho})\, \hat{a}_{q\sigma} e^{iqx}, \quad \zeta_q = \sqrt{\frac{\hbar\epsilon_0\omega_q}{2L}}, \qquad (1)$$

where the mode frequency, the photon annihilation op-

erator, and the quantization length are denoted by ω_q, $\hat{a}_q$, and L, respectively. Due to the spatial confinement [2, 10], the summation over the polarizations σ generally involves both transverse and longitudinal components. The electric field $\mathbf{E}^+$ in the waveguide may then be integrated using standard techniques of quantum optics [19], and expressed as a sum of the incident $\mathbf{D}_F^+$ and the scattered field,

$$\epsilon_0 \mathbf{E}^+(\mathbf{r}) = \mathbf{D}_F^+(\mathbf{r}) + \int d^3r' \, \mathsf{G}(\mathbf{r},\mathbf{r}') \, \mathbf{P}^+(\mathbf{r}') \,, \qquad (2)$$

$$\mathsf{G}(\mathbf{r},\mathbf{r}') = \frac{ik}{2} \, e^{ik|x-x'|} \mathsf{M}(k;\boldsymbol{\varrho},\boldsymbol{\varrho}') \,, \qquad (3)$$

where the electric polarization $\mathbf{P}^+(\mathbf{r}) = \sum_{ge} \mathbf{P}_{ge}^+(\mathbf{r}) = \sum_{ge} \mathbf{d}_{ge} \, \psi_g^\dagger(\mathbf{r}) \psi_e(\mathbf{r})$ acts as a radiation source. We have introduced the atomic field operators for the electronic ground and excited states $\psi_g(\mathbf{r})$ and $\psi_e(\mathbf{r})$, with the Zeeman levels included in the indices g and e when applicable, and the dipole matrix element $\mathbf{d}_{ge} = \mathcal{D} \sum_\sigma \hat{\mathbf{e}}_\sigma \mathcal{C}_{g,e}^{(\sigma)}$ for the atomic transition $|e\rangle \to |g\rangle$. Here the summation is over the circularly polarized unit vectors $\hat{\mathbf{e}}_\sigma$, $\mathcal{C}_{g,e}^{(\sigma)}$ denote the Clebsch-Gordan coefficients, and $\mathcal{D}$ is the reduced dipole matrix element. The polarization of the scattered light is determined by the tensor $\mathsf{M}(k;\boldsymbol{\varrho},\boldsymbol{\varrho}')$ that accounts for the projection to the transverse mode $\hat{\mathbf{u}}_{q\sigma}(\boldsymbol{\varrho})$ and the radial position $\boldsymbol{\varrho}'$ of the radiating atom. For instance, if the atoms with a complex level structure are trapped outside a nanofiber where the gradient of the evanescent field in the radial direction is large, the contribution of the longitudinal polarization can be significant leading to 'chiral', axial-direction-dependent emission [2, 10]. We have assumed that there is a dominant frequency $\Omega = kc$ of the driving light and, for simplicity of notation, here and in the rest of the paper we have written all operators in the "slowly varying" picture by explicitly factoring out the dominant frequency component $\mathbf{D}^+ \to e^{-i\Omega t}\mathbf{D}^+$, $\mathbf{P}^+ \to e^{-i\Omega t}\mathbf{P}^+$, etc. Owing to a single-mode nature of the waveguide, the radiation kernel $\mathsf{G}(\mathbf{r},\mathbf{r}')$ has the form of a 1D propagator [20] that does not lead to attenuation of the light propagating in the axial direction.

In order to solve the scattered field in Eq. (2), the equation of motion for $\mathbf{P}_{ge}^+$ can be derived analogously to the full field-theoretical treatment of the 3D electrodynamics [21], even while keeping the general hyperfine-level and polarization structure. However, in the following we assume that the atoms are tightly confined in the radial direction at the center of the waveguide ($\varrho = 0$), such that the effect of the radial dependence of the field mode on the atoms may be ignored, and that it is sufficient to consider scalar equations for each polarization component. We may then only consider a two-level system and replace $|\hat{\mathbf{u}}_q(\varrho \simeq 0)|$ by the inverse of the characteristic length scale of the radial light mode confinement. We take the radial light intensity profile to be a Gaussian with the $1/e$ width ξ_ϱ, such that $u(\varrho \simeq 0) = 1/\sqrt{\pi}\xi_\varrho$. Furthermore, we integrate over the radial dependence of the atomic polarization and density and, for simplicity of notation, assume that they have the same radial profile.

This results in an effective 1D theory [22] with the replacement $\pi\xi_\varrho^2 \mathbf{D}_F^+(\mathbf{r}) \to \tilde{D}_F^+(x)$, etc., where the radiation kernel G becomes a Green's function for the 1D Helmholtz equation $G(x-x') = ike^{ik|x-x'|}/2\pi\xi_\varrho^2$ [23]. The scattered field then depends on the scalar polarization $P^+ = \mathcal{D}\mathcal{C}_{ge}\psi_g^\dagger\psi_e$, and in the limit of low light intensity we obtain for the expectation value of the steady-state polarization $P_1 \equiv \langle P^+ \rangle$

$$P_1(x) = \alpha\rho\tilde{D}_F^+(x) + \eta_\delta \int dx' e^{ik|x-x'|} P_2(x;x') \,, \qquad (4)$$

where we have defined a single atom polarizability in a 1D waveguide as $\alpha = -2\gamma_w/[k(\delta + i\gamma_t)]$ in terms of the radiative linewidth $\gamma_t = \gamma_l + \gamma_w$ that depends on the radiative losses out of the waveguide γ_l and on the decay rate into the waveguide $\gamma_w = k\mathcal{D}^2/2\pi\xi_\varrho^2\hbar\epsilon_0$. The detuning of Ω from the atomic resonance is denoted by δ, the atom density by ρ, and $\eta_\delta \equiv \gamma_w/(i\delta - \gamma_t) = i\alpha k/2$.

Now, the polarization P_1 depends on the two-atom correlation function $P_2(x;x') = \langle \psi_g^\dagger(x) P^+(x') \psi_g(x) \rangle$. Analogously, for P_2 we obtain the steady-state solution

$$P_2(x_1;x_2) = \alpha\rho(x_1,x_2)\tilde{D}_F^+(x_2) + \eta_\delta e^{ik|x_1-x_2|} P_2(x_2;x_1) + \eta_\delta \int dx_3 \, e^{ik|x_2-x_3|} P_3(x_1,x_2;x_3) \,, \qquad (5)$$

where $\rho(x_1,x_2)$ denotes the ground-state atom pair correlation function that in the low light-intensity limit is unaffected by the driving light. In Eq. (5), P_2 depends on the three-body correlation function $P_3(x_1,x_2;x_3)$ for a polarization density at x_3, and ground-state atoms at x_1 and x_2. The three-atom correlation function P_3 in turn depends on four-atom correlations, etc., leading to the hierarchy of equations for the correlation functions.

After the rescaling the electromagnetic fields the cooperative response of atoms in a 1D waveguide closely resembles a 1D model electrodynamics [20] that described a hypothetical system consisting of continuously distributed 2D planes of atomic dipole moments in which case the radiators are discrete only in the direction of the light propagation. The one change is that we have specifically introduced the loss rates due to spontaneous emission out of the waveguide, and thus address an actual experimentally relevant physical system.

The second term in Eq. (5) describes repeated exchanges of a photon between atoms at x_1 and x_2. Such *recurrent* scattering processes [21, 24] between nearby atoms are responsible for light-induced correlations between the atoms. The hierarchy can be solved exactly by means of stochastic simulations where the positions of the atoms are sampled from a probabilistic ensemble that corresponds to the position correlations between

the atoms in the absence of the driving light [20]. In each stochastic realization of discrete atomic positions $\{x_1, x_2, \ldots, x_N\}$, we solve for the coupled set of classical electrodynamics equations for point dipoles that account for the polarization density $\sum_j \mathfrak{P}^{(j)}\delta(x - x_j)$, where $\mathfrak{P}^{(j)}$ denotes the excitation dipole of the atom j. The coupled-dipole equations for the steady-state solution in the present system read

$$\mathfrak{P}^{(j)} = \alpha \tilde{D}_F^+(x_j) + \eta_\delta \sum_{l\neq j} e^{ik|x_j - x_l|}\mathfrak{P}^{(l)}\,, \qquad (6)$$

where each dipole amplitude is driven by the incident field and the scattered field from all the other $N-1$ dipoles. Once all $\mathfrak{P}^{(j)}$ are calculated, the scattered fields in each realization may be obtained from $\epsilon_0 E_{\rm sc}^+(x) = ik\sum_l \exp(ik|x-x_l|)\mathfrak{P}^{(l)}/2$, and the total field equals the incoming field plus the scattered field. Finally, evaluating the ensemble average over many sets of atomic positions with the correct probability distribution generates the exact solution to the optical response of stationary atoms with a given atom statistics in the low-excitation limit [20]. The applicability of the simulations extends beyond atoms, since similar methods can be employed, e.g., in nanoresonator systems [25, 26].

The coupled dynamics for the atoms and light confined inside the waveguide exhibits characteristic behavior of 1D electrodynamics; for instance, for an exact resonant excitation the first atom can reflect all the light [20]. The single-atom transmission and reflection amplitudes equal

$$t^{(1)} = \frac{(\gamma_w - \gamma_t) + i\delta}{i\delta - \gamma_t}, \quad r^{(1)} = \frac{\gamma_w}{i\delta - \gamma_t}\,, \qquad (7)$$

with the single-atom power transmission and reflection coefficients given by $T^{(1)} = |t^{(1)}|^2$ and $R^{(1)} = |r^{(1)}|^2$. The total reflection occurs for suppressed photon losses, $\gamma_w = \gamma_t$. It is a generic phenomenon of 1D scattering – e.g., the origin of the Tonks gas behavior of impenetrable bosonic atoms in strongly confining 1D traps [27].

The hierarchy of equations represents light-induced correlations between the atoms that result from the recurrent scattering. In mean-field theory (MFT) such correlations are ignored. Next, we construct MFT solutions by specifically neglecting all recurrent scattering events, indicating that no photon scatters more than once by the same atom. For N atoms this means that each atom in a row simply passes on the same fraction of light and the transmission coefficient is given in terms of the single-atom transmission amplitude (7) as $t_{\rm mft}^{(N)} = \langle t^{(1)}\rangle^N$. Here we show that the MFT result can dramatically fail when light-induced correlations between the atoms become important. To model an atom cloud we solve the light transmission through the waveguide when the atomic positions are stochastically distributed. A cold classical atomic ensemble or an ideal Bose-Einstein condensate can be analyzed by sampling independent random atomic positions, while simulations in the quantum degenerate regime require one to synthesize a stochastic ensemble of atomic positions that generates the proper position correlations. We illustrate the latter by considering a metrologically important fermionic correlations (a zero-temperature fermionic gas or an impenetrable bosonic Tonks gas) in which case the stochastic ensemble in each run is generated with the Metropolis algorithm [28].

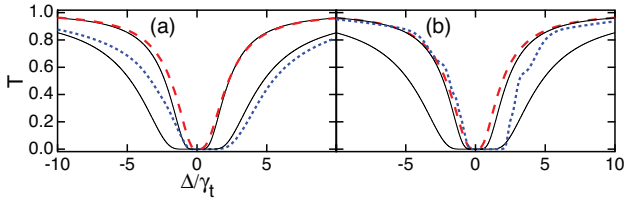

FIG. 1. Light-induced correlation effects between the atoms in transmitted light intensity T through the waveguide. The full numerical solution at atom densities $\rho k^{-1} = 2$ (dashed line) and 8 (dotted line) vs the corresponding MFT results (solid lines) for T as a function of the detuning of the incident light from the single atom resonance. The increased deviations indicate the growing importance of recurrent scattering. (a) Classical atoms that are uncorrelated before the light enters the sample; (b) fermionic atoms.

In Fig. 1 we show the exact simulation results with the corresponding MFT solution for different atom densities. At low densities the exact solution – that by definition fully incorporates all light scattering – coincides with the approximate MFT analysis that neglects all recurrent scattering processes and treats the atoms as independent. As the atom density gets higher the MFT solution becomes increasingly inaccurate, indicating the emergence of light-induced correlations between the atoms. It is perhaps surprising that an ensemble with a uniform density– such as a random distribution of classical atoms or, alternatively, a delocalized condensate wavefunction–exhibits correlated optics. Such a system mimics a continuous optical medium with a uniform refractive index [23], yet the light is still able to establish correlations between atoms, violating the standard continuous-medium optics.

The presence or absence of correlations due to recurrent scattering processes, as in Fig. 1, may be understood by considering fluctuations in the light propagation phases between the adjacent atoms. We adapt localization analysis using transfer matrices [17], originally introduced for 1D electric conductivity [22]. The MFT description $t_{\rm mft}^{(N)}$ becomes accurate whenever the transmission amplitude for N atoms at random positions factorizes into independent-atom contributions, $\langle t_{1,2,\ldots,N}^{(N)}\rangle = \langle t^{(1)}\rangle^N$, where $t^{(1)}$ is given by Eq. (7). (Alternatively, we can describe the factorization in terms of the N-atom optical thickness [22].) To determine the validity of MFT it is sufficient to consider a two-atom subsystem that can be recursively generalized to the N-atom case. For two

atoms we find

$$\langle t_{12}^{(2)} \rangle = \Big\langle \frac{t_2^{(1)} t_1^{(1)}}{1 - \sqrt{R_1^{(1)} R_2^{(1)}} e^{i\phi}} \Big\rangle . \tag{8}$$

The denominator can be represented as a geometric series where each subsequent term includes one additional recurrent scattering event between the atom pair [22]. The phase $\phi = \varphi_1 + \varphi_2 + 2kx_{12}$ ($x_{12} = x_2 - x_1$) consists of the light propagation phase $2kx_{12}$ from atom 1 to atom 2 and back, and the contributions $\varphi_j = \arctan(\delta_j/\gamma_t)$ from the atomic reflectance that are sensitive to the detunings of the driving light from the atomic resonance δ_j.

As may be seen by doing the average on the right-hand side of Eq. (8), MFT results, with the decoupling of the transmission amplitudes between the two atoms $\langle t_{12}^{(2)} \rangle \simeq t_1^{(1)} t_2^{(1)}$, if the propagation phases are distributed evenly over $[0, 2\pi)$ [22]. In fact, when the density is sufficiently low, $\rho \ll \pi/k$, so that for the characteristic interatomic separation $\ell = 1/\rho$ we have the propagation phase $2\ell k \gg 2\pi$, for random atomic positions the propagation phase for two adjacent atoms is distributed approximately evenly over $[0, 2\pi)$, and light-induced correlations are suppressed. At higher ρ the interatomic separation between the adjacent atoms is no longer large enough for the propagation phases to be random. Consequently, the light-induced correlations are not canceled out and we observe deviations from MFT. Analogously to the 3D case [16] the relevant length scale is $1/k$.

The cancelation of the effect of recurrent scattering may also occur at high densities in an inhomogeneously-broadened hot atom vapor due to the Doppler shifts of the resonance frequencies. In Eq. (8) the detunings δ_j also appear in the single atom transmission $t_j^{(1)}$ and reflectance $r_j^{(1)}$ [Eq. (7)]. If δ_j have a sufficiently broad distribution, then averaging over the velocity distribution of the atoms eliminates the recurrent scattering, and MFT becomes valid. The relevant energy scale for the Doppler broadening is the resonance linewidth of the atoms, and MFT is valid whenever the temperature is high enough such that $k\sqrt{k_B T/m} \gg \gamma_t$ [22].

In anticipation of ultracold many-body physics in hybrid waveguide systems, we extend calculations to quantum degenerate ensembles where the atoms still form an optical medium with a uniform density but they are no longer randomly distributed. If the atomic positions are correlated as a result of fermionic fluctuations, the short-range Fermi repulsion between the atoms creates an additional bias in the distribution of the propagation phases. We then find more dramatic violation of the MFT predictions [Fig. 1]. Evidently the phase in the denominator of Eq. (8) is less easily randomized away, leading to the strengthening of correlations in light propagation, resonance line narrowing, and suppressed superradiance.

Even though photonic crystal waveguide experiments strive toward low loss rate of photons from the waveguide,

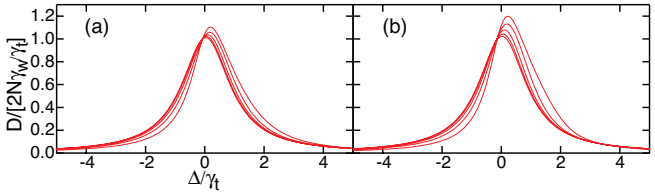

FIG. 2. Scaled optical thickness $-\langle \ln T_{12\ldots N}^{(N)} \rangle / (2N\gamma_w/\gamma_t)$ as a function of the detuning of light from the atomic resonance for $\gamma_w/\gamma_t = 0.4$, 0.2, 0.1, 0.05, and 0.025 (curves from top to bottom) for (a) initially uncorrelated classical atoms; (b) degenerate fermionic atoms ($L = 2\lambda$, $N = 32$). For $\gamma_w/\gamma_t \to 0$, all cases converge to the MFT result of $\gamma_t^2/(\gamma_t^2 + \delta^2)$.

nanofiber systems typically have $\gamma_w/\gamma_t \ll 1$. With high losses, the number of multiple scattering events any single photon can undergo inside the waveguide is limited. To leading order in γ_w/γ_t, we obtain for the two-atom transmission $T_{12}^{(2)} \simeq T_1^{(1)} T_2^{(1)} + \mathcal{O}(\gamma_w^2/\gamma_t^2)$, indicating the recovery of the MFT results. In Fig. 2 we show the numerically simulated light transmission for different loss rates. In the limit $\gamma_w/\gamma_t \to 0$ the curves converge toward the MFT result, but notable deviations can be identified even in the case of strong losses.

We calculated the MFT results by treating the transmission of each atom independently and then taking the product of the transmissions of independent atom. We may also neglect the recurrent scattering and light-induced correlations between the atoms directly in the hierarchy of equations by factorizing the correlation function $P_2(x; x') \simeq \rho(x) P_1(x')$ in Eq. (4). This truncates the hierarchy, provides closed equations from which P_1 and the scattered fields may be solved, and leads to an effective-medium MFT. It was shown in a 3D system that in the low atom-density limit the factorization reproduces the "cooperative Lamb shift" (CLS) that Friedberg *et al.* [29] have calculated for various 3D geometries of atomic ensembles. The experimental measurement of CLS has attracted considerable interest with nuclei [30], ions [31], and CLS was recently qualitatively verified in hot [32] and low-density [33] atomic vapors. In systems where the light-induced correlations between the emitters become strong, CLS prediction can fail [16]. Here the factorization $P_2(x; x') \simeq \rho(x) P_1(x')$ in Eq. (4) gives CLS of the 1D waveguide in the limit of asymptotically small density [22]

$$\Delta_{\rm CLS} = \frac{\gamma_w \rho}{2k} \left(1 - \frac{\sin 2Lk}{2Lk} \right) . \tag{9}$$

The oscillatory behavior corresponds to the etalon effect due to the sample thickness. In 1D physical and practical constraints conspire to make it difficult to verify the result (9) numerically, but for judiciously chosen parameters we get close [Fig. 3(a)]. Moreover, in numerical computations the resonance shift is found to be on the order of $\gamma_w \rho/(2k)$ for a wide range of parameters. This

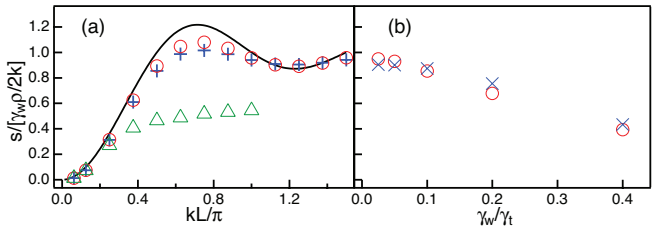

FIG. 3. Frequency shift s of the maximum of the light intensity transmitted through the waveguide. (a) The shift (solid line) as predicted by the "cooperative Lamb shift" model (9), and the full numerics (at $\rho = 32\,k/\pi$) for $\gamma_w/\gamma_t = 0.01$ (circles), 0.02 (crosses), and 0.1 (triangles) as a function of sample thickness. (b) Variation of line shift with waveguide loss rate. These are the shifts of the curve maxima in Fig. 2 for classical (circles) and fermionic (crosses) atoms.

is illustrated in Fig. 3(b) for the line shifts in Fig. 2.

In conclusion, nanophotonic waveguides can naturally enhance light-mediated collective response in atomic ensembles. Collective optical phenomena find applications, e.g., in engineering superradiance [8], narrow spectral linewidths [25, 34], enhanced extinction [35], subwavelength excitations [36], lasers [37], controlling line shifts [16, 30–32, 38], and in 1D waveguides in the studies of Anderson-localized modes of light [13]. Here we analyzed light transmission through an atomic ensemble in a waveguide. The light-induced correlations due to recurrent scattering were identified both in simulations and in a transfer matrix analysis. The validity of MFTs was characterized in terms of atom density, thermal broadening, and photon loss rate. We also pointed out that quasi-1D waveguide systems may exhibit perhaps unexpected frequency shifts – an observation that may be relevant in sensing and metrology [4].

We acknowledge support from NSF, Grant Nos. PHY-0967644 and PHY-1401151, and EPSRC.

[1] A. Goban, C. L. Hung, S. P. Yu, J. D. Hood, J. A. Muniz, J. H. Lee, M. J. Martin, A. C. McClung, K. S. Choi, D. E. Chang, O. Painter, and H. J. Kimble, Nat Commun **5**, 3808 (2014).

[2] R. Mitsch, C. Sayrin, B. Albrecht, P. Schneeweiss, and A. Rauschenbeutel, Nat Commun **5**, 5713 (2014).

[3] E. Vetsch, D. Reitz, G. Sagué, R. Schmidt, S. T. Dawkins, and A. Rauschenbeutel, Phys. Rev. Lett. **104**, 203603 (2010); A. Goban, K. S. Choi, D. J. Alton, D. Ding, C. Lacroûte, M. Pototschnig, T. Thiele, N. P. Stern, and H. J. Kimble, Phys. Rev. Lett. **109**, 033603 (2012); R. Yalla, M. Sadgrove, K. P. Nayak, and K. Hakuta, Phys. Rev. Lett. **113**, 143601 (2014); G. Epple, K. S. Kleinbach, T. G. Euser, N. Y. Joly, T. Pfau, P. S. J. Russell, and R. Löw, Nat Commun **5**, 4132 (2014).

[4] S. Okaba, T. Takano, F. Benabid, T. Bradley, L. Vincetti, Z. Maizelis, V. Yampol'skii, F. Nori, and H. Katori, Nat Commun **5**, 4096 (2014).

[5] D. E. Chang, A. S. Sorensen, E. A. Demler, and M. D. Lukin, Nat Phys **3**, 807 (2007); A. V. Akimov, A. Mukherjee, C. L. Yu, D. E. Chang, A. S. Zibrov, P. R. Hemmer, H. Park, and M. D. Lukin, Nature **450**, 402 (2007).

[6] J. Volz, M. Scheucher, C. Junge, and A. Rauschenbeutel, Nat Photon **8**, 965 (2014); T. G. Tiecke, J. D. Thompson, N. P. de Leon, L. R. Liu, V. Vuletic, and M. D. Lukin, Nature **508**, 241 (2014); H. Zoubi and H. Ritsch, New Journal of Physics **12**, 103014 (2010); F. Le Kien and K. Hakuta, Phys. Rev. A **79**, 013818 (2009); Z. Liao, X. Zeng, S.-Y. Zhu, and M. S. Zubairy, Phys. Rev. A **92**, 023806 (2015).

[7] J.-T. Shen and S. Fan, Phys. Rev. Lett. **95**, 213001 (2005); L. Zhou, Z. R. Gong, Y.-x. Liu, C. P. Sun, and F. Nori, Phys. Rev. Lett. **101**, 100501 (2008).

[8] A. Goban, C.-L. Hung, J. D. Hood, S.-P. Yu, J. A. Muniz, O. Painter, and H. J. Kimble, Phys. Rev. Lett. **115**, 063601 (2015).

[9] D. E. Chang, J. I. Cirac, and H. J. Kimble, Phys. Rev. Lett. **110**, 113606 (2013); J. S. Douglas, H. Habibian, C. L. Hung, A. V. Gorshkov, H. J. Kimble, and D. E. Chang, Nat. Photon. **9**, 326 (2015); A. González-Tudela, C. L. Hung, D. E. Chang, J. I. Cirac, and H. J. Kimble, Nat. Photon. **9**, 320 (2015); D. Roy, Scientific Reports **3**, 2337 EP (2013).

[10] J. Petersen, J. Volz, and A. Rauschenbeutel, Science **346**, 67 (2014).

[11] I. Söllner, S. Mahmoodian, S. L. Hansen, L. Midolo, A. Javadi, G. Kiršanskė, T. Pregnolato, H. El-Ella, E. H. Lee, J. D. Song, S. Stobbe, and P. Lodahl, Nat Nano **10**, 775 (2015).

[12] P. Genevet, D. Wintz, A. Ambrosio, A. She, R. Blanchard, and F. Capasso, Nat Nano **10**, 804 (2015).

[13] L. Sapienza, H. Thyrrestrup, S. Stobbe, P. D. Garcia, S. Smolka, and P. Lodahl, Science **327**, 1352 (2010).

[14] M. J. Hartmann, F. G. S. L. Brandao, and M. B. Plenio, Nat Phys **2**, 849 (2006).

[15] A. Wallraff, D. I. Schuster, A. Blais, L. Frunzio, R. S. Huang, J. Majer, S. Kumar, S. M. Girvin, and R. J. Schoelkopf, Nature **431**, 162 (2004).

[16] J. Javanainen, J. Ruostekoski, Y. Li, and S.-M. Yoo, Phys. Rev. Lett. **112**, 113603 (2014); J. Javanainen and J. Ruostekoski, Opt. Express **24**, 993 (2016).

[17] P. W. Anderson, D. J. Thouless, E. Abrahams, and D. S. Fisher, Phys. Rev. B **22**, 3519 (1980); R. Landauer, Philosophical Magazine **21**, 863 (1970); M. V. Berry and S. Klein, European Journal of Physics **18**, 222 (1997).

[18] E. A. Power, *Introductory Quantum Electrodynamics*, Mat. Phys. Ser., Vol. 24 (Longmans, London, 1964); C. Cohen-Tannaudji, J. Dupont-Roc, and G. Grynberg, *Photons and Atoms: Introduction to Quantum Electrodynamics* (John Wiley & Sons, New York, 1989).

[19] P. W. Milonni and P. L. Knight, Phys. Rev. A **10**, 1096 (1974); P. W. Milonni, *The Quantum Vacuum: An Introduction to Quantum Electrodynamics*, 1st ed. (Academic Press, London, 1994).

[20] J. Javanainen, J. Ruostekoski, B. Vestergaard, and M. R. Francis, Phys. Rev. A **59**, 649 (1999).

[21] J. Ruostekoski and J. Javanainen, Phys. Rev. A **55**, 513 (1997).

[22] See Supplemental Material for additional details regarding technical background information.

[23] M. Born and E. Wolf, *Principles of Optics*, 7th ed. (Cambridge University Press, Cambridge, UK, 1999); J. D. Jackson, *Classical Electrodynamics*, 3rd ed. (Wiley, New York, 1999).

[24] O. Morice, Y. Castin, and J. Dalibard, Phys. Rev. A **51**, 3896 (1995); L. Chomaz, L. Corman, T. Yefsah, R. Desbuquois, and J. Dalibard, New Journal of Physics **14**, 005001 (2012); S. E. Skipetrov and I. M. Sokolov, Phys. Rev. Lett. **112**, 023905 (2014).

[25] S. D. Jenkins and J. Ruostekoski, Phys. Rev. Lett. **111**, 147401 (2013).

[26] S. D. Jenkins and J. Ruostekoski, Phys. Rev. B **86**, 085116 (2012).

[27] M. Olshanii, Phys. Rev. Lett. **81**, 938 (1998).

[28] D. M. Ceperley, Rev. Mod. Phys. **67**, 279 (1995).

[29] R. Friedberg, S. R. Hartmann, and J. T. Manassah, Physics Report **7**, 101 (1973); J. T. Manassah, Adv. Opt. Photon. **4**, 108 (2012).

[30] R. Röhlsberger, K. Schlage, B. Sahoo, S. Couet, and R. Rüffer, Science **328**, 1248 (2010).

[31] Z. Meir, O. Schwartz, E. Shahmoon, D. Oron, and R. Ozeri, Phys. Rev. Lett. **113**, 193002 (2014).

[32] J. Keaveney, A. Sargsyan, U. Krohn, I. G. Hughes, D. Sarkisyan, and C. S. Adams, Phys. Rev. Lett. **108**, 173601 (2012).

[33] S. Roof, K. Kemp, M. Havey, and I. Sokolov, "eprint arxiv:1603.07268," (2016); M. Araújo, I. Krešić, R. Kaiser, and W. Guerin, "eprint arxiv:1603.07204," (2016).

[34] B. Luk'yanchuk, N. I. Zheludev, S. A. Maier, N. J. Halas, P. Nordlander, H. Giessen, and C. T. Chong, Nat. Mater. **9**, 707 (2010).

[35] R. J. Bettles, S. A. Gardiner, and C. S. Adams, Phys. Rev. Lett. **116**, 103602 (2016).

[36] F. Lemoult, G. Lerosey, J. de Rosny, and M. Fink, Phys. Rev. Lett. **104**, 203901 (2010); S. D. Jenkins and J. Ruostekoski, Phys. Rev. A **86**, 031602(R) (2012); T. S. Kao, S. D. Jenkins, J. Ruostekoski, and N. I. Zheludev, Phys. Rev. Lett. **106**, 085501 (2011).

[37] J. G. Bohnet, Z. Chen, J. M. Weiner, D. Meiser, M. J. Holland, and J. K. Thompson, Nature **484**, 78 (2012).

[38] S. D. Jenkins, J. Ruostekoski, J. Javanainen, R. Bourgain, S. Jennewein, Y. R. P. Sortais, and A. Browaeys, Phys. Rev. Lett. **116**, 183601 (2016).